ACS APPLIED MATERIALS & INTERFACES

Letter

www.acsami.org

# Magnetic Elastomers for Stretchable Inductors

Nathan Lazarus,*[,†] Chris D. Meyer,[†] Sarah S. Bedair,[†] Geoffrey A. Slipher,[†] and Iain M. Kierzewski[‡]

[†]U.S. Army Research Laboratory, 2800 Powder Mill Road, Adelphi, Maryland 20783, United States

[‡]General Technical Services, 2800 Powder Mill Road, Adelphi, Maryland 20783, United States

Supporting Information

**ABSTRACT:** In this work, silicone loaded with magnetic particles is investigated for creating a composite with higher permeability while still maintaining stretchability. Magnetic and mechanical properties are first characterized for composites based on both spherical and platelet particle geometries. The first magnetic-core stretchable inductors are then demonstrated using the resulting ferroelastomer. Solenoid inductors based on liquid metal galinstan are then demonstrated around a ferroelastomeric core and shown to survive uniaxial strains up to 100%. Soft elastomers loaded with magnetic particles were found to increase the core permeability and inductance density of stretchable inductors by nearly 200%.

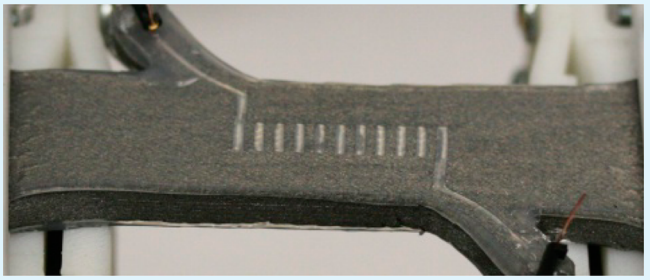

**KEYWORDS:** *composite materials, stretchable electronics, magnetic materials, inductors*

The field of stretchable electronics has become increasingly important in recent years, with uses including biomedical devices,[1] soft robotics,[2] and wearable systems.[3] Stretchable structures can survive repeated strains of tens to hundreds of percent. This property becomes important for sensor on a surface such as human skin,[1] an inherently stretchable substrate that can reach strains up to 100%.[4] Because connections for data and power are likely failure points in stretchable systems, highly deformable inductors have been developed for wireless power[5,6] and communications.[1] Stretchable inductors have been fabricated using wavy rigid conductors,[1,5] microcracked metal films,[7] and liquid metals,[6,8,9] all in a nonmagnetic stretchable substrate. Many nonstretchable inductive systems utilize high permeability magnetic materials to increase inductance density. Magnetic backplanes may be incorporated to improve coupling between wireless power coils.[10] However, the magnetic materials in these systems are typically rigid and poorly suited for stretchable electronics.

Ferroelastomers are stretchable polymers such as silicone that are loaded with magnetic particles. The resulting composite retains most of the mechanical properties of the elastomer while adding a magnetic response, including relative permeability greater than one, because of the embedded particles. The most prominent use of ferroelastomers has been for magnetorheological elastomers (MRE), elastomers with tunable mechanical behavior based on applied magnetic field.[11] The field creates a force on individual particles that resists mechanical strain, resulting in increased effective stiffness. Other uses of ferroelastomers include electromagnetic shielding[12] and microstructure actuation.[13] A survey of the mechanical and magnetic behavior of representantive silicone-based ferroelastomers is shown in Table S1 in the Supporting Information.

This work investigates the use of ferroelastomers for stretchable electronics. By incorporating magnetic particles, the first magnetic-core stretchable inductor is demonstrated, a solenoid based on liquid metal around a ferroelastomer core. Using ferroelastomers results in higher permeability and resulting inductance density compared with nonmagnetic elastomers. With magnetic particles, unstretched inductance was increased up to 2.9 times that of an inductor with the original elastomer core, while surviving strains of up to 100%. Galinstan (melting point −19 °C) was chosen for the electrodes to minimize resistance, because liquid inductor traces have been demonstrated to survive strains of 200% with cross-sections as large as millimeters.[8] The elastomer used was the soft silicone Ecoflex 00−30 (Smooth-On), with a breakage strain of 900% and an elastic modulus at low strain of approximately 125 kPa.[14]

Ferroelastomers were created using one of two different commercially obtained magnetic particles, molypermalloy powder (MPP) (Spang and Co.) and Sendust (Steward LP987). Molypermalloy is a nickel−iron−molybdenum alloy (79% Ni, 17% Fe, 4% Mo) with bulk relative permeability of 20 000.[15] MPP is made by grinding bulk molypermalloy and sieving to a desired mesh size; as a result, the 400-mesh (maximum particle size 37 $\mu$m) powder used in this work consisted of a range of sizes, primarily in the tens of microns, with a roughly spherical or boulder shape (Figure 1a). This mesh/particle size was chosen as the smallest size commercially available for MPP. Sendust (85% iron, 9% silicon, 6%

**Received:** March 12, 2015
**Accepted:** May 6, 2015
**Published:** May 6, 2015





DOI: 10.1021/acsami.5b02189
*ACS Appl. Mater. Interfaces* 2015, 7, 10080−10084

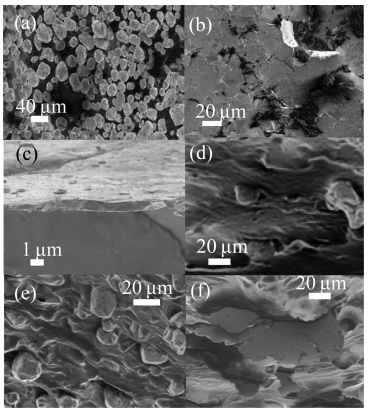


**Figure 1.** SEM images of (a–c) magnetic particles before coating: (a) MPP, (b, c) Sendust, and (d–f) after mixing in elastomer: (d) 60% and (e) 80% by weight MPP and (f) 20% by weight Sendust.

aluminum) has a similarly high relative permeability of 16 000 to 36 000.[16] The Sendust powder consisted of thin platelets, flat sheets (Figure 1b) with thickness approximately 1 $\mu$m (Figure 1c). Both Sendust and MPP are used for powder cores, inductor cores based on highly packed magnetic powders with a small quantity of binding polymer used for structure and isolation.[17] To maximize permeability, the polymer in powder core inductors is generally less than 10% by volume (3–4% by weight),[17] too low for practical ferroelastomers.

Molypermalloy powder and Sendust were mixed into liquid silicone precursors before curing to create the magnetic composite. Adding powders results in an increase in the viscosity of the mixture. The maximum usable concentration occurs when the liquid becomes too viscous to be poured for molding. The MPP mixture remained pourable up to 80% molypermalloy by weight, while the Sendust became too viscous above 20% by weight. The difference in viscosity is likely due to particle shape, with long thin Sendust platelets affecting the shear forces within the fluid more than the smaller spherical MPP. Dense powders also gradually settle during curing, resulting in a surface layer in the elastomer largely void of the filler material. To minimize settling, we rapidly cured the elastomer at 85 °C on a hot plate, with final cure occurring in less than 30 min.

Magnetic composites can be treated as magnetic circuits, where magnetic flux is inversely proportional to the closed path line integral of magnetic field by a quantity defined as reluctance, a magnetic circuit analog to electrical resistance. Both MPP and Sendust have a relative permeability in the tens of thousands, compared with one for the nonmagnetic silicone. Highly magnetic particles behave as effective "shorts," approximately zero reluctances, and are surrounded by regions of high-reluctance silicone (magnetically free space). The overall permeability is therefore set not by the permeability of the particles themselves, but by the width and number of gaps between neighboring particles. The average number of gaps and width of each defines the total distance through nonmagnetic silicone that the magnetic field must pass through within the core, known as the "distributed air gap" of the inductor,[18] and the ratio between the total core length and this value is approximately the relative permeability. As packing density increases, the spacing between particles falls. Each ferroelastomer was cut after curing and examined using a scanning electron microscope to estimate particle spacing. With 60% MPP by weight (16% by volume), the gap between neighboring particles is tens of microns (Figure 1d). As the MPP loading increases to 80% by weight (33% by volume), this gap drops to less than ten micrometers (Figure 1e). The Sendust platelets are more isolated because the maximum loading is only 20% by weight (4% by volume) (Figure 1f). However, because the sheets of Sendust are highly anisotropic, very long, and thin, the number of gaps between particles to create a complete magnetic path will also be shorter than the more spherical MPP. No additional magnetic field was applied during curing, so there is no preferred alignment for the Sendust platelets. Sheets of Sendust that happen to be aligned with a magnetic field will effectively short out large regions of silicone.

To extract the relative permeability, we encapsulated commercial air core inductors (Coilcraft 2929SQ-501, nominal inductance 500 nH) in Sendust- and MPP-based ferroelastomers and compared to a similar inductor in nonmagnetic silicone. The precise orientation, sizing, and positioning of the individual particulate is effectively random; creating an exact model of the permeability is impossible. Instead, effective medium theory was used, where assumptions about the general shape and distribution of particles are used to approximate the behavior. The Maxwell Garnett model[19] assumes ellipsoid particles, evenly distributed and far enough apart that particles are only weakly interacting,[21] and is valid for the relatively low fill fractions in this work. Within these assumptions, permeability follows the relationship[20]

$$\frac{\mu_{\text{eff}} - \mu_1}{\mu_{\text{eff}} + 2\mu_1} = f\frac{\mu_2 - \mu_1}{\mu_2 + 2\mu_1} \quad (1)$$

where $\mu_{\text{eff}}$, $\mu_1$, and $\mu_2$ are permeabilities of the composite, surrounding medium, and particle inclusions, respectively, and $f$ is the volume fill fraction of the inclusions. The shape of an ellipsoid also acts to reduce the effective magnetic moment within a particle, according to a geometric term known as the demagnetizing factor. The demagnetizing factors of the three axes must sum to one.

The boulder-shaped molypermalloy can be treated as roughly spherical; because spherical particles are isotropic, the demagnetizing factors for each axis will be equal to 1/3, resulting in no impact from the orientation of individual particles. Figure 2a shows measured relative permeability for different loading fractions of MPP, along with expected results using the model. The average particle diameter used in the model was 22.3 $\mu$m, estimated by measuring the size distribution of particles optically. The Sendust particles, on the other hand, are very asymmetric, flat platelets with average diameter 66 $\mu$m and thickness 1 $\mu$m.[22] Cumulative size distributions for each are provided inFigure S1 in the Supporting Information. The demagnetization factor for a platelet is very close to zero in plane, and approximately one normal to the plate (assuming a flat disk with the Sendust dimensions, 0.163 and 0.968 for in plane and out of plane respectively).[23] The orientation therefore makes a large difference in the resulting permeability. If all the plates are normal to the magnetic field, almost no silicone is magnetically shorted by the particles, and the relative permeability will be close to 1. When plates are completely aligned with the applied field, the permeability will be maximized. In the Sendust-loaded composite, platelets are randomly ordered, with no preferential alignment direction; some plates are aligned in parallel with the field, resulting in shorting of long lengths of silicone, whereas


DOI: 10.1021/acsami.5b02189
ACS Appl. Mater. Interfaces 2015, 7, 10080–10084

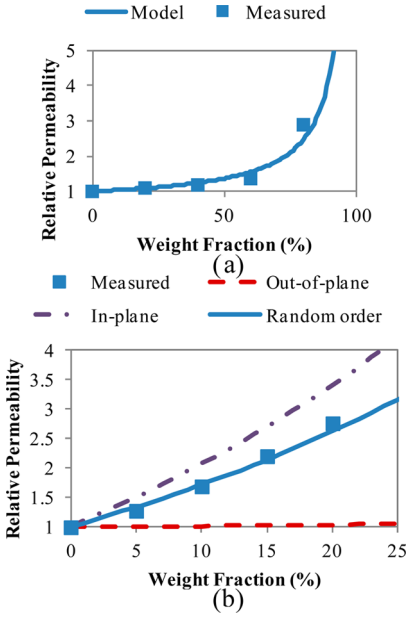


**Figure 2.** Relative permeability of (a) MPP and (b) Sendust ferroelastomer with varying loading fraction of magnetic particles.

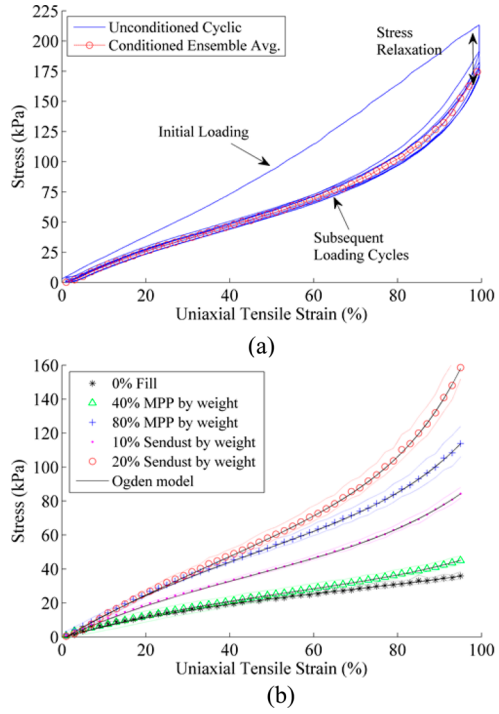


**Figure 3.** (a) Cyclic loading data for 20% by weight Sendust ferroelastomer and (b) stress−strain curves of MPP- and Sendust-based ferroelastomers.

others will be angled and have lower impact. In the model, this randomization is incorporated by assuming a third are aligned with each axis because of the lack of a preferential direction. Measured permeability for the Sendust composite closely follows the expected permeability for random ordering (Figure 2b).

Adding filler particles to elastomers such as natural rubber has been done for centuries for the purposes of both reinforcement and cost reduction, most commonly with carbon black or silica particles.[24] As the fraction of particulate increases, the effective stiffness of the ferroelastomer will rise because of two effects: the weighted combination of the stiffness of the two constituents is higher, and the particles provide additional cross-linking sites that restrict the mobility of the polymer chains.[25] Because the magnetic particles are orders of magnitude stiffer than the polymer, the blend results in a gradual increase in mechanical strength and effective elastic modulus of the bulk composite material as the volume fraction of particulate increases. As with the magnetic behavior, particle shape plays an important role. Long narrow platelets, with a high surface area to volume ratio, interact more strongly with the neighboring polymer than spheres with similar volume.

The combined strain-softening and strain-hardening behaviors of hyperelastic rubber materials such as silicone are well-described by the Ogden model.[26,27] The elastomer is assumed to be incompressible, with a Poisson's ratio approximately 0.5, and thus the volume of the material is conserved during deformation. During quasi-static uniaxial strain testing, the elastomers were found to experience significant stress relaxation, with the initial loading cycle having a stiffer response before softening to approach a steady-state elastically reversible behavior in subsequent loading cycles (Figure 3a). Because the Ogden model assumes that the stress−strain curve is completely reversible, the samples were first conditioned by applying multiple loading cycles to reach consistent behavior. An ensemble average of multiple stress−strain curves covering multiple cycles and multiple specimens was obtained after conditioning ferroelastomers loaded with 40 and 80% MPP as well as 10 and 20% Sendust (Figure 3b). A four-parameter Ogden model was then obtained using a nonlinear regression on the ensemble averages for each formulation. Increasing particle volume fractions results in two primary changes in the quasi-static mechanical behavior of the bulk material: (1) effective stiffness increases and (2) the strain softening and strain hardening effects are amplified. For the same mass loading fraction, both effects are much more pronounced in the Sendust loaded samples. For example, 20% Sendust by weight has a stress−strain curve that tracks closely to the stress−strain curve for 80% MPP by weight (Figure 3b). The effect of the large platelet area counteracts the difference in volume loading. This effect parallels the previously mentioned effect on viscosity observed in the precured ferroelastomers. The Sendust-based ferroelastomers are thus mechanically similar to the MPP-based elastomer with comparable permeability, although with far lower mass density and resulting sample weight in the final composite.

In a stretchable magnetic core, one of the most important characteristics is the change in effective permeability when the composite is deformed. Stretching a ferroelastomer results in a change in the relative position of rigid particles within the magnetic composite. Because magnetic particles are orders of magnitude more rigid than the surrounding silicone, the deformation occurs primarily in the soft elastomer. As the composite is stretched, the particles move farther apart along the strain axis, resulting in a larger spacing between the individual particles in the direction of stretching. Poisson's effect leads to a corresponding decrease in particle spacing in the directions normal to the direction of stretching. The resulting increase in the effective gap along the magnetic core and corresponding reduction in cross-section geometry is expected to result in a drop in permeability as the core is stretched.


DOI: 10.1021/acsami.5b02189
ACS Appl. Mater. Interfaces 2015, 7, 10080−10084

In our previous work,[9] a technique was developed for fabricating a nonmagnetic core solenoid inductor using liquid metal (summarized in the Supporting Information). 3D printed molds (Figure S2 in the Supporting Information) are used to create multilayer open channels in soft silicone, which are then sealed by bonding to partially cured silicone. Galinstan injected into the channels forms stretchable conductive traces. Using the same technique, a magnetic core solenoid was fabricated by substituting ferroelastomer for the molded layer. Because the inductance of a solenoid is primarily dependent on the permeability within the core, nonmagnetic Ecoflex was used for the top and bottom sealing layers. This allows the traces to be observed during liquid metal fill and testing, because the partially transparent silicone becomes dark and opaque when loaded with magnetic particles. Both inductors with applied strain direction along and perpendicular to the core direction were tested to determine if the permeability became anisotropic during stretching.

Solenoids with ferroelastic cores consisting of 20% Sendust and 80% MPP were tested using a uniaxial testing setup (Figure 4a). The inductance of a coil is dependent on geometry, allowing use as a hyperelastic strain gauge.[8] A solenoid stretched along its core axis drops in inductance, while the same strain perpendicular to the core axis increases the inductance. When the magnetic core inductor is stretched, the inductance (Figure 4c, e) varies both due to the changing geometry as well as the variation in the effective permeability of the ferroelastomer. For strains parallel to the core, both materials exhibit comparable behavior, with measured inductances being almost indistinguishable between the two composites at each tested value of strain. However, for large strains perpendicular to the core, the Sendust-based inductor exhibits lower inductance than the comparable MPP sample. Because the magnetic fields of a solenoid are concentrated in the core, the inductance is proportional to the magnetic permeability of the core material.[28] Approximate permeability (Figure 4d, f) can therefore be calculated by dividing by the nonmagnetic core inductance at a given strain value. Permeability drops for both perpendicular and parallel mechanical strains in both materials; the lower inductance for the perpendicular strains in the Sendust material is reflected in a larger drop in the relative permeability. The drop in permeability for both directions of mechanical strain results from an increase in the average particle spacing in the material. In an incompressible material such as an elastomer at moderate strains, particle spacing increases linearly in the direction of applied strain, while along the other two axes it drops more slowly according to a square root relation.[8] When the particles are initially randomly distributed, this difference in behavior results in most particles moving farther apart (more than 80% of possible particle positions for the strains in this work, as shown in the numerical example in the Supporting Information and Figure S3). A five cycle loading test to 40% maximum applied uniaxial strain was also performed on each of the two ferroelastomers, finding no clear change in inductance density and permeability behavior with cycling (Figure S4 in the Supporting Information).

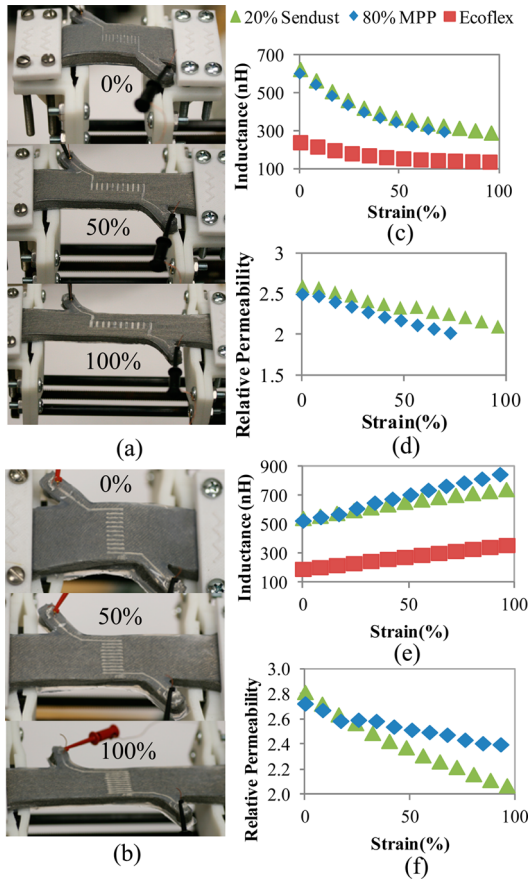


**Figure 4.** Mechanical testing of 20% Sendust inductor for strain (a) along and (b) perpendicular to core axis and measured inductance and estimated permeability for applied strain (c, d) along inductor core and (e, f) perpendicular to core axis.

Using magnetic materials such as the ferroelastomers in this work allows larger inductance densities to be reached in stretchable inductors. Although the relative permeability remains small relative to traditional core materials, it represents a nearly 200% increase in the inductance of the solenoid compared to nonmagnetic silicone. With platelet-type particulate, this increase requires only a 25% increase in mass density of the elastomer. We believe that stretchable magnetic-core inductors are an important development for improving communication and power systems in highly compliant systems. The stretchable magnetic-core solenoid demonstrated in this work would be ideal for tuning the mechanical properties in MRE-based soft robotic grippers. The same material is also well-suited as magnetic backplanes for stretchable wireless power.

## ■ ASSOCIATED CONTENT

### Supporting Information

Additional information and figures as noted in the text. Brief experimental section containing details on ferroelastomer preparation and inductor characterization. The Supporting Information is available free of charge on the ACS Publications website at DOI: 10.1021/acsami.5b02189.

## ■ AUTHOR INFORMATION

### Corresponding Author

*E-mail: nathan.lazarus2.civ@mail.mil.

### Author Contributions

The manuscript was written through contributions of all authors. All authors have given approval to the final version of the manuscript.



DOI: 10.1021/acsami.5b02189
ACS Appl. Mater. Interfaces 2015, 7, 10080−10084

### Notes

The authors declare the following competing financial interest(s): A related patent filing is in preparation.

## ■ ACKNOWLEDGMENTS

The authors thank Steward Advanced Materials for providing the Sendust and the Magnetics division of Spang and Co. for providing the molypermalloy powder.

## ■ REFERENCES

(1) Kim, D.; Lu, N.; Ma, R.; Kim, Y.; Kim, R.; Wang, S.; Wu, J.; Won, S. M.; Tao, H.; Islam, A.; Yu, K. J.; Kim, T.; Chowdhury, R.; Ying, M.; Xu, L.; Li, M.; Chung, H.; Keum, H.; McCormick, M.; Liu, P.; Zhang, Y.; Omenetto, F. G.; Huang, Y.; Coleman, T.; Rogers, J. A. Epidermal Electronics. *Science* **2011**, *333*, 838−843.

(2) Lu, N.; Kim, D. Flexible and Stretchable Electronics Paving the Way for Soft Robotics. *SoRo* **2013**, *1*, 53−62.

(3) Yun, D.; Yun, K. Woven Piezoelectric Structure for Stretchable Energy Harvester. *Electron. Lett.* **2013**, *49*, 65.

(4) Bethke, K. The Second Skin Approach: Skin Strain Field Analysis and Mechanical Counter Pressure Prototyping for Advanced Spacesuit Design. *M.S. Thesis*, Massachusetts Institute of Technology, Cambridge, MA, June 2005.

(5) Kim, R.; Tao, H.; Kim, T.; Zhang, Y.; Kim, S.; Panilaitis, B.; Yang, M.; Kim, D.; Jung, Y. H.; Kim, B. H.; Li, Y.; Huang, Y.; Omenetto, F. G.; Rogers, J. A. Materials and Designs for Wirelessly Powered Implantable Light-Emitting Systems. *Small* **2012**, *8*, 2812−2818.

(6) Qusba, A.; RamRakhyani, A. K.; So, J. H.; Hayes, G. J.; Dickey, M. D.; Lazzi, G. On the Design of Microfluidic Implant Coil for Flexible Telemetry System. *IEEE Sens. J.* **2014**, *14*, 1074−1080.

(7) Harris, J.; Graudejus, O.; Wagner, S. Elastically Stretchable Insulation and Bilevel Metallization and its Application in a Stretchable RLC Circuit. *J. Electron. Mater.* **2011**, *40*, 1335−1344.

(8) Fassler, A.; Majidi, C. Soft-matter Capacitors and Inductors for Hyperelastic Strain Sensing and Stretchable Electronics. *Smart Mater. Struct.* **2013**, *22*, 055023.

(9) Lazarus, N.; Meyer, C. D.; Bedair, S. S.; Nochetto, H.; Kierzewski, I. M. Multilayer Liquid Metal Stretchable Inductors. *Smart Mater. Struct.* **2014**, *23*, 085036.

(10) Zheng, Y.; Sun, X.; Li, Z.; Li, X.; Zhang, H. Flexible MEMS Inductors Based on Parylene-FeNi Compound Substrate for Wireless Power Transmission System in *Proc. NEMS 2013* Suzhou, China April 2013, 1002−1005.

(11) Varga, Z.; Filipcsei, G.; Zrinyi, M. Magnetic Field Sensitive Functional Elastomers with Tuneable Elastic Modulus. *Polymer* **2006**, *47*, 227−233.

(12) Kong, I.; Ahmad, S. H.; Abdullah, M. H.; Hui, D.; Yusoff, A. N.; Puryanti, D. Magnetic and Microwave Absorbing Properties of Magnetite-Thermoplastic Natural Rubber Nanocomposites. *J. Magn. Magn. Mater.* **2010**, *322*, 3401−3409.

(13) Lagorce, L. K.; Brand, O.; Allen, M. G. Magnetic Microactuators Based on Polymer Magnets. *J. Microelectromech. Syst.* **1999**, *8*, 2−9.

(14) Park, Y.; Majidi, C.; Kramer, R.; Berard, P.; Wood, R. J. Hyperelastic Pressure Sensing with a Liquid-Embedded Elastomer. *J. Micromech. Microeng* **2010**, *20*, 125029.

(15) Chin, G. Y.; Wernick, J. H. Soft Magnetic Metallic Materials. In *Ferromagnetic Materials*; Wohlfarth, E. P., Ed.; North Holland: New York, 1986; Vol. 2.

(16) Helms, H. H.; Adams, E. Sendust Sheet-Processing Techniques and Magnetic Properties. *J. Appl. Phys.* **1964**, *35*, 871−872.

(17) Shokrollahi, H.; Janghorban, K. Soft Magnetic Composite Materials (SMCs). *J. Mater. Process. Technol.* **2007**, *189*, 1−12.

(18) Skarrie, H. Design of Powder Core Inductors. *Ph.D. Thesis*, Lund University, Lund, Sweden,2001.

(19) Maxwell Garnett, J. C. Colours in Metal Glasses and in Metallic Films. *Philos. Trans. R. Soc., A* **1904**, *203*, 385−420.

(20) Yang, R. B.; Hsu, S. D.; Lin, C. K. Frequency-dependent Complex Permittivity and Permeability of Iron-Based Powders in 2−18 GHz. *J. Appl. Phys.* **2009**, *105*, 07A527.

(21) Koledintseva, M. Y.; DuBroff, R. E.; Schwartz, R. W. A Maxwell Garnett Model for Dielectric Mixtures Containing Conducting Particles at Optical Frequencies. *Prog. Electromagn. Res.* **2006**, *63*, 223−242.

(22) *Magnetic Powders Datasheet*; Steward Advanced Materials: Chattanooga, TN, 2013.

(23) Chen, D.; Pardo, E.; Sanchez, A. Radial Magnetometric Demagnetizing Factor of Thin Disks. *IEEE Trans. Magn.* **2001**, *37*, 3877−3880.

(24) Anifantis, N. K.; Georgantzinos, S. K.; Giannopoulos, G. I.; Kakavas, P. A. Elastomer Macrocomposites. In *Advances in Elastomers II: Composites and Nanocomposites*; Visakh, P. M., Thomas, S., Chanda, A. Kp., Mathew, A. P., Eds.; Springer: Berlin-Heidelberg, Germany, 2013.

(25) Bergstrom, J. S.; Boyce, M. C. Mechanical Behavior of Particle Filled Elastomers. *Rubber Chem. Technol.* **1999**, *72*, 633−656.

(26) Ogden, R. W. Large Deformation Isotropic Elasticity: On the Correlation of Theory and Experiment for Incompressible Rubber-like Solids. *Proc. R. Soc. London, Ser. A* **1972**, *326*, 565−584.

(27) Ogden, R. W.; Saccomandi, G.; Sgura, I. Fitting Hyperelastic Models to Experimental Data. *Comput. Mech.* **2004**, *34*, 484−502.

(28) Ahn, C. H.; Allen, M. G. A New Toroidal-Meander Type Integrated Inductor with a Multilevel Meander Magnetic Core. *IEEE Trans. Magn.* **1994**, *30*, 73−79.



DOI: 10.1021/acsami.5b02189
*ACS Appl. Mater. Interfaces* 2015, 7, 10080−10084